Progress In Electromagnetics Research B, Vol. 25, 241–259, 2010

MULTI-FLOOR INDOOR POSITIONING SYSTEM USING BAYESIAN GRAPHICAL MODELS

A. S. Al-Ahmadi, A. I. Omer, M. R. Kamarudin and T. A. Rahman

Wireless Communication Centre
Universiti Teknologi Malaysia
Skudai, Johor 81310, Malaysia

Abstract—In recent years, location determination systems have gained a high importance due to their rule in the context aware systems. In this paper, we will design a multi-floor indoor positioning system based on Bayesian Graphical Models (BGM). Graphical models have a great flexibility on visualizing the relationships between random variables. Rather than using one sampling technique, we are going to use multiple sets each set contains a collection of sampling techniques, the accuracy of each set will be compared with each other.

1. INTRODUCTION

Recent advances in communication technologies have a great impact on location determination systems. Location determination systems are deployed in almost every building, from hospitals were the location of patients and doctors or any medical equipment can be determined, or sending information to customers based on their location, to organize the traffic and reducing congestion in the highways.

RADAR [1] is an in-building RF-based user location and tracking system uses the nearest neighbor in signal space (NNSS) technique to predict the user's location. NNSS uses the online received signal strength (RSS) to search for the closest match stored in the radio map during the offline phase by minimizing the Euclidean distance between the physical location of the user and the estimated location. The system depends on empirical data collection to build a radio map for the test bed. The radio map contains *tuples* in the form

Received 12 August 2010, Accepted 7 September 2010, Scheduled 14 September 2010
Corresponding author: A. S. Al-Ahmadi (abdullah.alahmadi@ymail.com).

(t, x, y, d) where t represents the timestamp, (x, y) is the coordinates of user's location and d is the orientation of the user's facing (north, south, east or west). RADAR's accuracy is effected by the size of NNSS used, training points and samples size in the online phase. The system also uses signal propagation modeling approach to build the radio map, the goal was to reduce the system dependence on empirical data. The authors ignored the Floor Attenuation Factor (FAF) which was proposed by [2] and adopted the Wall Attenuation Factor (WAF) instead. They discovered that there is an inverse relationship between the amount of additional attenuation and the number of walls separating the transmitter and the receiver. The accuracy of the system was about 2–3 m.

Horus [3], a probabilistic WLAN location determination system which was designed with the goal of high accuracy and low computational cost. The system uses a technique called location-clustering in order to reduce the computational cost. Having a small computational cost systems is an important aspect in designing a location determination system, it enables such systems to be implemented in smaller devices. The system also operates in two stages: an Off-line phase where the radio map is built using a *Joint Clustering* technique where the test bed is divided into clusters, and any two locations are in the same cluster if they are both covered by the same APs, a discrete space estimator estimates the RSS histogram for each AP at each location, and an On-line phase, where the actual estimating of the user's location happen by finding the location x which maximize the probability of getting that location given a signal strength vector s.

In [4], the authors presented a hybrid indoor positioning method that uses ray-tracing model for modeling the multipath effects. The system works in two stages, in the first stage, it uses the direction of arrival (DOA) and RSS to build a database of fingerprints, while in the second stage it determines the position of the mobile station by computing the Euclidean distance values of DOA and RSS with the values stored in the database.

In [5], the authors proposed an indoor location determination system that uses non line of sight (NLOS) scheme and one bound scattering paths. The system is a two step Determination and Selection (two step DS), which in the first step it calculates the estimated location from a cluster of Line of Possible Mobile Device location (LPMD). In the second step, the system tries to find the shortest Euclidean distance from the centroid. The system adjusts the Line of Sight (LOS) measurement of the Angle of Arrival (AOA) and TOA to the real values.

The disadvantage of the above systems is that they do not work in multi-floor environments. Most indoor positioning system based on TOA or AOA metrics requires a sophisticated devices to measure time or angle. Since our system was designed to work with off-the-shelf components, which means no additional requirements were needed other than an Access Point (AP) and a WiFi enabled device. Moreover, TOA location determination systems uses the TOA measurement of the first path to determine the location which in turn is difficult to be calculated accurately in indoor environments [6].

For a list of systems and methods used in indoor location determination [7–10].

2. RSS PROPERTIES IN INDOOR ENVIRONMENTS

In order for us to design an ideal indoor positioning system, studying the properties of RSS in indoor environments is a crucial aspect in this study. Signal strength in indoor environments is difficult to predict due to multipath effects such as reflection, diffraction and scattering [11]. In this section, we are going to study different RSS properties that will effect our system.

2.1. Distribution of RSS in Indoor Environment

The average RSS in indoor environments is considered to be log-normally distributed [12]. Figure 1 shows the histogram of RSS for three access points during work hours in the first floor of Wireless Communication Centre (WCC) building. The signal fingerprints were collected at fixed location for five minutes with one second time interval. The figure shows that each histogram is unique and different from each other. Table 1 shows different values for the mean, median mode and standard deviation. Figure 1 proves that the RSS at fixed location does not follow a normal distribution but a log-normal distribution due to the similarity between the statistical values for each

Table 1. Statistical values for three APs at fixed location in the first floor.

Statistics	AP 1	AP 2	AP 3
Mean (dBm)	−103.7	−67.6	−68.3
Median (dBm)	−101.0	−66.0	−67.0
Mode (dBm)	−102	−66	−65
Std. Deviation (dB)	4.7	3.2	3.7

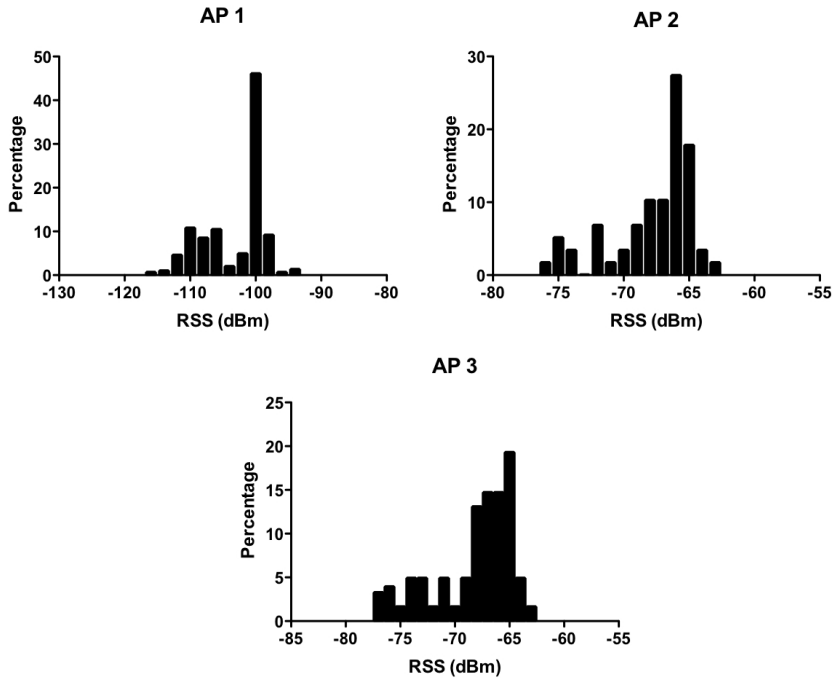

Figure 1. RSS distribution at fixed locations from three access points.

AP. Moreover, the data did not pass D'Agostino-Pearson Omnibus test since the P values for each test were too small.

2.2. Using RSS to Infer Locations

In our system, RSS will be used as reference to infer the indoor location. A test was conducted to show the possibility of using RSS, Figure 2 shows the variation of RSS measurements recorded from five APs while walking through a track in the first floor at WCC building. The signal received at any given location is higher when that location is close to the AP, and weaker when it is far away. This shows the feasibility of using RSS as a location fingerprint.

Figure 2 also shows the uniqueness of RSS tuples. Each RSS tuples at each location are different. This indicates that RSS fingerprints are the best choice for inferring indoor locations. The figure shows also the small variation of RSS against the distance which indicates the distance between each training point should not be relatively small.

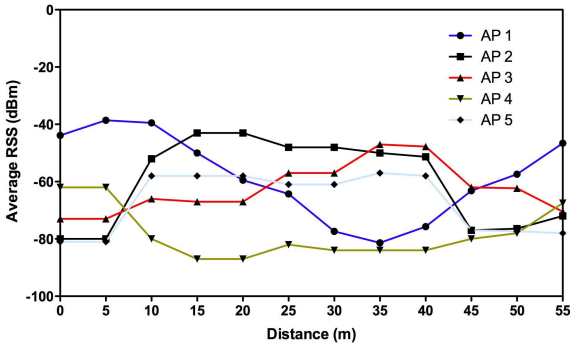

Figure 2. RSS while walking inside WCC from five APs.

Table 2. RSSs statistics from two APs at two different floors.

Statistics	AP2 Floor 1	AP2 Floor 2	AP5 Floor 1	AP5 Floor 2
Mean	−52.13	−72.24	−72.18	−47.21
Median	−52.00	−72.00	−72.00	−47.00
Std. Deviation	2.475	1.014	3.592	1.467
Min	−57.00	−76.00	−82.00	−51.00
Max	−43.00	−69.00	−46.00	−44.00

2.3. Multi-floor Effect

According to [13], a concrete floor may reduce the RSS between 15 dB and 35 dB. In order to investigate the effect of floors in the indoor environment, we performed a set of measurements at two fixed locations referred as $A1$ in Figure 4(a) and $A2$ in Figure 4(b), $A1$ and $A2$ are vertically and symmetrical locations.

At each location, we have collected RSSs for five minutes with 1 second sampling time from $AP2$ in first floor and $AP5$ in the second floor.

Figure 3 and Table 2 show the effect of floor in our test bed, for $AP2$ the floor attenuation is 20.11 dB and 24.97 dB for $AP5$. The average floor attenuation to the RSS from an AP implemented in different floor is 22.5 dB.

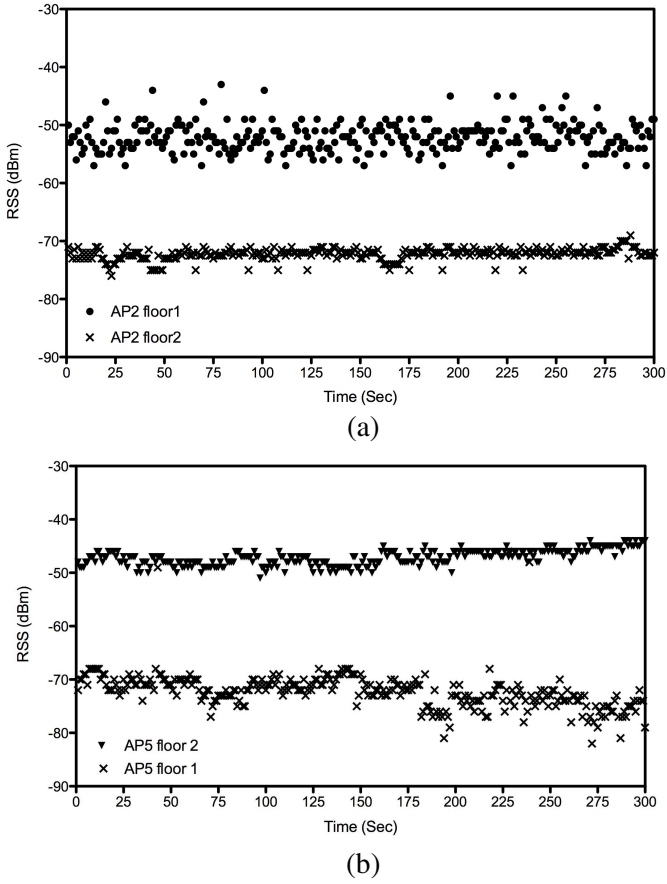

Figure 3. Multi- oor effect at two fixed locations from (a) AP2 and (b) AP5.

2.4. Multiple Diffraction from Window Frames

In addition to the effect of FAF, [14] suggests that there are another two factors that most likely have an effect on signal propagation in a multi-floor environment:

(i) Multiple diffraction from window frames.

(ii) Reflection from scattered signals from adjacent buildings.

In this paper, we will ignore the effect of adjacent buildings due to floors layout constrains. Multiple diffraction is caused by the propagated signal being diffracted at window frame edges at locations

(a) (b)

Figure 4. Two floor plans showing (a) three APs in first floor and (b) two APs in the second floor.

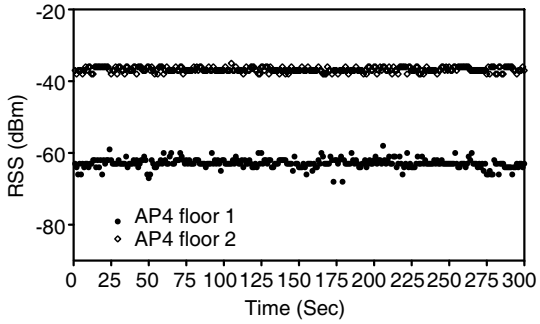

Figure 5. The effect of FAF at locations near to the window frames.

Table 3. The floor attenuation factor effect in the centre of the floors and next to windows.

	Centre 1st floor	Centre 2nd floor	Window
Mean (dBm)	−52.13	−47.21	−36.79
Median (dBm)	−52	−47	−37.00
FAF (dB)	20.11	24.97	26.1

in different floors. In Figure 12, we show the effect of multiple diffraction from window frames. RSS fingerprints were recorded at location $B1$ in first floor and $B2$ in the second floor for five minutes. The AP is located in the second floor near a glass window. From Figure 5 and Table 3, the FAF appears to be the dominant factor while the diffraction from windows has no effect.

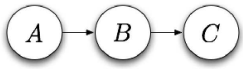

Figure 6. A simple graphical model.

3. BAYESIAN GRAPHICAL MODELS

A *graphical model* is a statistical model representing a set of conditional independence relationships [15]. Figure 6 shows a simple graphical model. The nodes A, B and C represent a random variable while the edges represent relationships between those random variables. We say any node is a *parent* when there is an arrow pointing out of that node to a *descendant* node. In Figure 6, node A is a parent for node B, and node B is a parent for node C. We may also say that a node is a child when there is an arrow pointing to that node. Therefore, node B is a child of node A, and C is a child of B. A parent node A is considered to be the direct influence on its children, C is independent of its non-descendants given its parent [16]. The joint density of all random variables for BGM in Figure 6 is:

$$P(A, B, C) = P(A)\, P(B \mid A)\, P(C \mid B)$$

in other words:

$$P(X) = \prod_{x \in X} P(x \mid parent(x)) \tag{1}$$

In BGM, most of the random variables represent the variability of the observed data, while some variables represent the unobserved data that affects the observed variables [17].

3.1. Markov Chain Monte Carlo Sampling Techniques

Monte Carlo (MC) methods such as rejection sampling and importance sampling techniques do not work well in complex situations. Markov Chain Monte Carlo (MCMC) works in more complicated problems. In MCMC, we want to draw a large number of samples from the posterior distribution, these samples can be then used to estimate the posterior mean. In this section, we will give a brief description of 3 sampling techniques that were used in our model.

3.1.1. Gibbs Sampler

Gibbs sampler [18] is an univariate sampler that picks the value of each random variable from its conditional probability distribution given all other quantities [19].

If we have a simple regression model:

$$s_i \sim N\left(b_0 + b_1 X_1 + \ldots + b_z X_z, \tau\right) \tag{2}$$

the Gibbs sampler works by sampling each of the conditional distribution one at a time, Algorithm 1 shows the steps of Gibbs sampler [20]:

Algorithm 1 The Gibbs Sampler algorithm

(i) Set initial values for parameters b_i

(ii) For $t = 1, \ldots, T$ repeat

(a) Set $b = b^{(t-1)}$

(b) For $i = 1, \ldots, z$

1. update b_i from $b_i \sim f\left(b_i | b_{\setminus i}, S\right)$ repeat

(c) Set $b^t = b$

(d) Save it for $t + 1$ iteration

$$\begin{aligned} b_0 &\sim P\left(b_0 | b_1, \ldots, b_z, \tau, S\right) \\ b_1 &\sim P\left(b_1 | b_0, b_3, \ldots, b_z, \tau, S\right) \\ &\vdots \\ b_z &\sim P\left(b_z | b_0, b_3, \ldots, b_z - 1, \tau, S\right) \\ \tau &\sim P\left(\tau | b_0, \ldots, b_z, S\right) \end{aligned} \tag{3}$$

3.1.2. Metropolis-Hastings Sampler

Metropolis-Hasting was initiated by [21] as a generalization of the Metropolis algorithm which was introduced by [22]. Algorithm 2 shows the steps of a Metropolis-Hasting algorithm.

Algorithm 2 Metropolis-Hasting algorithm

(i) Set initial values for parameters b_i

(ii) For $t = 1, \ldots, T$ repeat

(a) Set $b = b^{(t-1)}$

(b) Generate new value b' from a proposal distribution $h\left(b' | b\right)$

(c) Calculate

$$\alpha = \min\left(1, \frac{f\left(b' | S\right) h\left(b | b'\right)}{f\left(b | S\right) h\left(b' | b\right)}\right)$$

(d) Update $b^{(t)} = b'$ with probability α, otherwise set $b^{(t)} = b$

3.1.3. Slice Sampler

Slice sampling [23] works by using a supportive variable v, and drawing samples from the joint distribution $Uniform\,(b, v)$ such that:

$$p\,(b, v) = \begin{cases} 1/B & \text{if } 0 \leq v \leq p\,(x) \\ 0 & \text{otherwise} \end{cases} \tag{4}$$

where $B = \int p\,(b)\,db$, and the marginal distribution over b is:

$$p\,(b) = \int p\,(b)\,dv = \int_0^{p(b)} \frac{1}{B}\,dv \tag{5}$$

Algorithm 3 Slice Sampler Algorithm

(i) Set $b = b^{(t-1)}$

(ii) For $i = 1, \ldots, n$

  (a) generate $v_i^{(t)} \sim Uniform\,(0, f\,(v_i|b))$

(iii) For $j = 1, \ldots, d$

  (a) update $b_j \sim f\,(b_j) \prod_{i=1}^{n} I\left(0 \leq v_i^{(t)} \leq f\,(v_i|b)\right)$

(iv) Set $b^{(t)} = b$

3.2. Burn-in Samples

Burn-in samples are samples that were initially generated and will be rejected in order to eliminate their effect on the posterior distribution, burn-in samples are not valid since Markov chain has not stabilized [20].

3.3. Ordered Over-relaxation

Over-relaxation [24] is used to improve the convergence of Gibbs sampler, it generates multiple random values at each iteration and chooses the one that is negatively correlated with the current value from a conditional distribution and then arranging these values in non-decreasing order.

4. MODEL AND MEASUREMENT SETUP

A single unshaded circle symbolizes a continuous stochastic node while the shaded node represents a discrete stochastic node, stochastic nodes are always assigned to a distribution, discrete stochastic nodes are

represented by a single shaded circle, while a double unshaded circle refers to a logical variable, and finally, single rectangular represents a constant.

4.1. Data Collection

In order to construct a radio map for our test bed, an offline data collection at specified locations was needed. NetStumbler [25], a free software for detecting signal strengths from APs was used. In addition to RSSs, NetStumbler can also record MAC, SSID, SNR and channel speed of each AP. Unfortunately, due to experiencing some difficulties with NetStumbler, like the inability to record the location of the fingerprint collected and not being able to operate in some operating systems, we developed *UTM WiFi Scanner,* a software that allows us to record RSSs, MAC address, SSID, channel and speed of each APs along with their (x, y) coordinates and z (the floor number). Our software is based on *inSSIDer* [26], an open source WLAN scanner written in C sharp language under Apache license.

We performed our test at WCC building at UTM, the building has two floors, first floor is about 36 m × 30 m and the second floor is approximately 21 m × 28 m, there are five D-Link DWL-2000AP APs, with operating frequency from 2.4 GHz to 2.4835 GHz, 3 in the first floor and 2 in the second floor, each AP has 15 dBm transmit power. Most of the building's walls are concrete and some walls are made of a plaster partition board, the wall thickness is about 15 cm and floor thickness is about 80 cm, Figure 4 show the building's floor plan. RSSs fingerprints were collected on a MacBook running Windows XP Service Pack 3 in Boot Camp. The laptop is equipped with AirPort Extreme card, the card supports IEEE 802.11 a/b/g/n standards.

Fingerprints were recorded at 21 locations in floor 1 and 9 locations in floor 2, at each location, we collected 20 RSS in 360° rotation with one second time interval during office work hours. In the off-line phase, the user clicks on displayed map in UTM WiFi Scanner, then the (X, Y, Z) coordinates of the user are saved in a file with the RSS, MAC, SSID, SNR values from each AP. Figure 7 shows UTM WiFi Scanner graphical user interface during data collection.

4.2. Our Model

Figure 8 show our mode which we are going to call it $WCC01$, it is based on model *M2* in [16], but we have modified our model to fit a multi-floor environment.

Nodes X_i, Y_i and Z_i represent the user's location at the ith training point. $\bar{x_j}$ and $\bar{y_j}$ are constant nodes which represent the

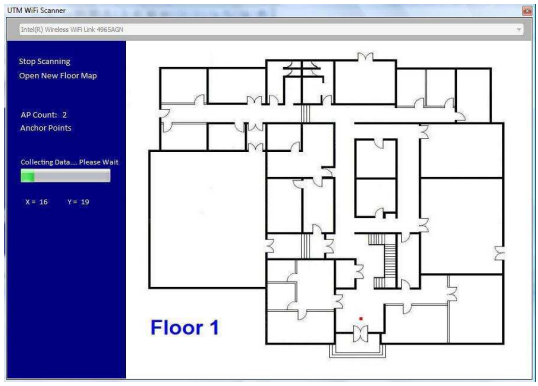

Figure 7. UTM WiFi Scanner GUI during data collection.

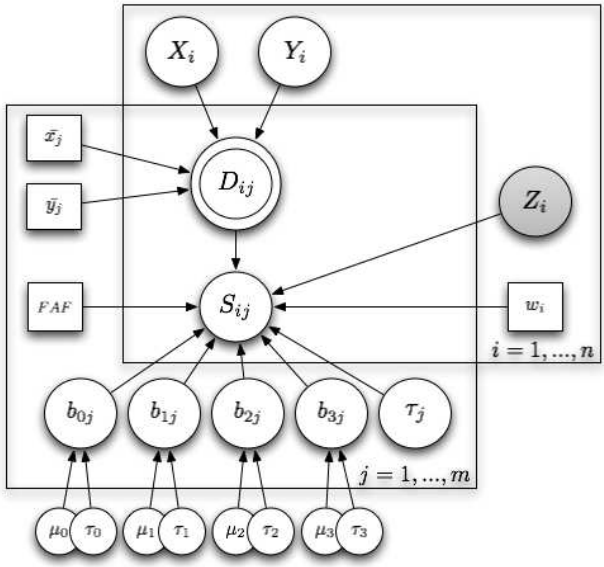

Figure 8. A Bayesian graphical model using WinBUGS plate notation. We call this model WCC01.

location of the jth AP. FAF is the floor attenuation factor. D_{ij} is the Euclidean distance between the location specified by (X_i, Y_i) and $(\bar{x_j},\bar{y_j})$, node S_{ij} represents the signal strength received at location (X_i, Y_i) from the jth AP. Node w_i takes 0 if RSS recorded at location (X_i, Y_i) and the jth AP were at the same floor and 1 otherwise.

The nodes are defined as follows:

$$\begin{aligned}
X_i &\sim U(0, L) \\
Y_i &\sim U(0, W) \\
Z_i &\sim DisU(1, N) \\
D_{ij} &= \log\left(1 + \sqrt{(X_i - \bar{x_j})^2 + (Y_i - \bar{y_j})^2}\right) \\
S_{ij} &\sim Norm(b_{0j} + (b_{1j} * D_{ij}) + (b_{2j} * Z_i) \\
&\quad +(b_{3j} * w_i * FAF), \tau_j), \quad i = 1, \ldots, n, \\
&\quad j = 1, \ldots, m, \\
b_{cj} &\sim Norm(\mu_c, \tau_c), \quad c = 1, 2, 3, 4, \\
\mu_c &\sim Norm(0, 1.0E-6), \quad c = 1, 2, 3, 4, \\
\tau_c &\sim Gamma(0.01, 0.01), \quad c = 1, 2, 3, 4.
\end{aligned}$$

L represents the length of the test bed while W is the width and N is the number of floors.

Since *WinBUGS* (Bayesian Inference Using Gibbs Sampler) does not support discrete uniform distribution, we had to construct our own distribution as a categorical distribution as follows:

$$\text{for } (i \text{ in } 1:30) \quad \{p[i] < -30 \qquad Z[i] \sim \text{dcat}(p[\,])\}$$

Categorical distribution is a generalization of Bernoulli distribution with sample space $\{1, 2, 3, \ldots, n\}$. It can be used in BUGS by:

$$x \sim \text{dcat}(p[\,]) \tag{6}$$

where

$$x = 1, 2, 3, \ldots, \dim(p)$$

4.3. Data Analysis

In order to compute the posterior distribution, we will use BUGS [27], a free software used to generate samples for the parameters of posterior distribution. Figure 9 shows two trace plots for X_i in Figure 9(a) and for Y_i in Figure 9(b), clearly the two random variables X_i and Y_i have converged since no patterns were observed, then we do not have to generate more samples.

We simulate using four sets of sampling methods as appear in Table 4. In Set 1, adaptive metropolis updater was used for random variables X_i and Y_i, a discrete slice updater was chosen for Z_i in the four steps, conjugate normal updater for b_{cj} and μ_c, and a conjugate gamma updater for random variable τ_c. In Set 2, adaptive metropolis updater was used for X_i, Y_i, b_{cj} and μ_c and a slice updater for τ_c,

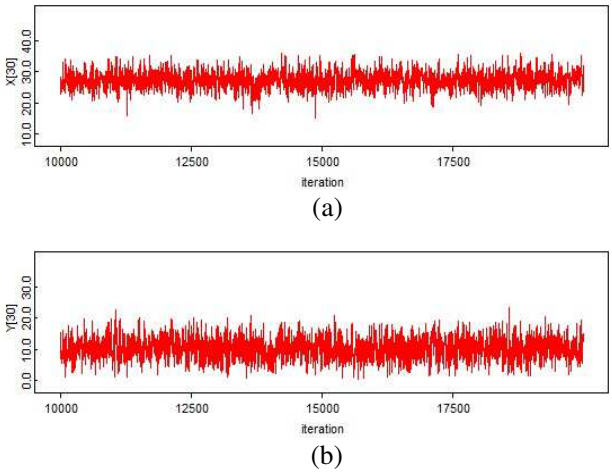

Figure 9. Trace plot of all stored values with no patterns observed for variables (a) $X[30]$ and (b) $Y[30]$.

Table 4. Four sets of sampling techniques used in our model.

	Set 1	Set 2	Set 3	Set 4
Adaptive Metropolis	*	*	*	
Conjugate normal	*		*	*
Conjugate gamma	*			
Slice		*	*	*
Discrete Slice	*	*	*	*

while in Set 3, adaptive metropolis also was chosen for X_i and Y_i, a conjugate normal form b_{cj} and μ_c and a slice updater for random variable τ_c, and finally in Set 4, a slice updater for X_i, Y_i and τ_c and a conjugate normal updater for b_{cj} and μ_c.

Figure 10 shows the visual estimation for variables of posterior probability function, $X[30]$ in 10(a), $Y[30]$ in 10(b) and $Z[30]$ in 10(c), a bell-shaped posterior distribution indicates that the MC chain has converged. Figure 11 shows the generated samples for variables for $X[30]$, $Y[30]$ in 11(a) and $Z[30]$ in 11(b). We got these results by running the MC chain 10,000 iterations with another 10,000 iteration for the burn-in period. We also tested our model with different FAF values to show its effect on location error, in Figure 12(a) shows the location error after running 10,000 iteration with four different FAF values and in Figure 12(b) after running 50,000 iteration. We noticed

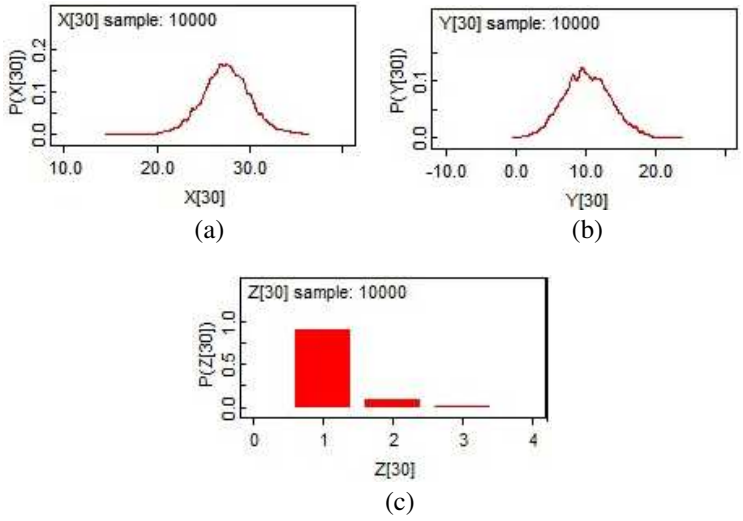

Figure 10. An approximate visual kernel estimate of the posterior distribution of random variables (a) $X[30]$, (b) $Y[30]$ and (c) $Z[30]$.

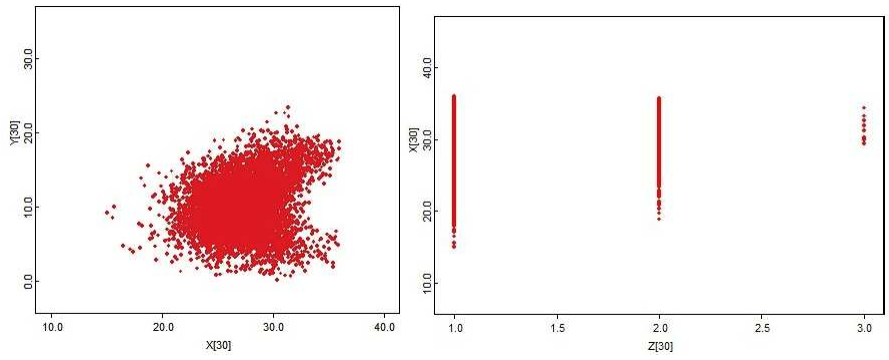

Figure 11. Generated samples using Gibbs sampler for (a) $X[30]$, $Y[30]$ and (b) $Z[30]$.

that the overall accuracy was increased while the number of iterations increased. We got better results with $FAF = 25\,\text{dB}$, the error mean at this value is about 3.8 m. In Figure 13, we show our results with each sets mention in Table 4 after choosing $FAF = 25\,\text{dB}$, we ran the MC chain for 100,000 iteration after discarding the first 10,000 iteration as burn-in samples. From Table 5, Set 1 of sampling techniques appears

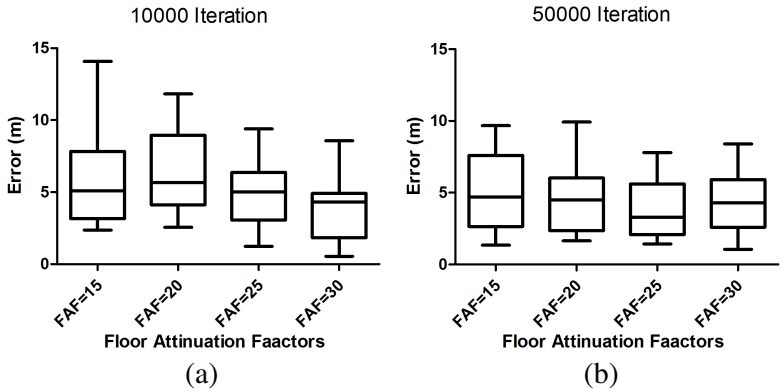

Figure 12. The effect of different FAF values and number of iterations on the estimated location error.

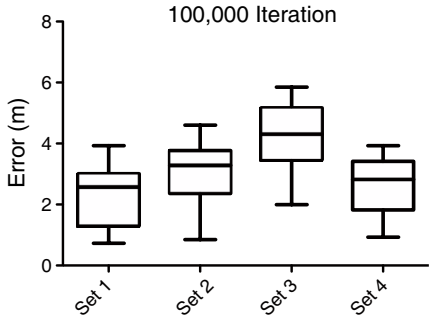

Figure 13. Location error results using the four sets with $FAF = 25$ dB after running the MC chain for 100,000 iteration and 10,000 iteration in burn-in period.

to give the most accurate results with mean error of 2.283 m and 75% percentile of 3 meters, while Set 3 gives the most inaccurate results by error mean of about 4.2 m and 75% percentile equal to 5.17 m.

In Table 6, we compare our results with similar off-the-shelf positioning systems, namely RADAR [1] and the Horus location determination system proposed by [3]. Although the dimensions of the first floor of our test bed is bigger than the test bed in [3], we were able to achieve almost the same accuracy with 70% less training points. Note that our 30 training points were collected in two floors.

Table 5. Location error in meters after running the MC chain for 100,000 iteration.

	Set 1	Set 2	Set 3	Set 4
Minimum	0.7304	0.8516	1.996	0.9312
75% Percentile	3.011	3.769	5.173	3.418
Maximum	3.929	4.600	5.848	3.927
Mean	2.283	3.084	4.193	2.671

Table 6. Comparison between different indoor positioning systems.

	RADAR	Horus	Our model
Floor Dimensions (m)	43.5×22.5	11.8×35.9	36×30
Number of Training Points	70	100	30
Accuracy (m)	3	2.1	2.3
Multi-Floor	No	No	Yes

5. CONCLUSION

In this paper, a Bayesian graphical model for multi-floor indoor positioning system was designed. First we studied the RSS properties that will affect the overall accuracy of our model, then we gave a brief review on the MCMC sampling techniques we used. Finally, we tested our model with four sets of MCMC sampling techniques and compared our results with two well known location determination systems. We were able to achieve accuracy of 2.3 m in a multi-floor environment with a small amount of training points.

REFERENCES

1. Bahl, P. and V. Padmanabhan, "RADAR: An in-building RF-based user location and tracking system," *IEEE INFOCOM*, Vol. 2, 775–784, Citeseer, 2000.
2. Seidel, S. and T. Rappaport, "914 MHz path loss prediction models for indoor wireless communications in multi oored buildings," *IEEE Transactions on Antennas and Propagation*, Vol. 40, No. 2, 207–217, 1992.
3. Youssef, M. and A. Agrawala, "The Horus location determination system," *Wireless Networks*, Vol. 14, No. 3, 357–374, 2008.

4. Tayebi, A., J. Gomez, F. Saez de Adana, and O. Gutierrez, "The application of ray-tracing to mobile localization using the direction of arrival and received signal strength in multipath indoor environments," *Progress In Electromagnetics Research*, Vol. 91, 1–15, 2009.
5. Seow, C. and S. Tan, "Localization of omni-directional mobile device in multipath environments," *Progress In Electromagnetics Research*, Vol. 85, 323–348, 2008.
6. Kanaan, M. and K. Pahlavan, "A comparison of wireless geolocation algorithms in the indoor environment," *IEEE Wireless Communications and Networking Conference*, 177–182, 2004.
7. Honkavirta, V., T. Perala, S. Ali-Loytty, and R. Piche, "A comparative survey of WLAN location fingerprinting methods," *6th Workshop on Positioning, Navigation and Communication WPNC*, 2009.
8. Liu, H., H. Darabi, P. Banerjee, and J. Liu, "Survey of wireless indoor positioning techniques and systems," *IEEE Transactions on Systems, Man, and Cybernetics, Part C: Applications and Reviews*, Vol. 37, No. 6, 1067–1080, 2007.
9. Pandey, S. and P. Agrawal, "A survey on localization techniques for wireless networks," *Journal — Chinese Institute of Engineers*, Vol. 29, No. 7, 1125, 2006.
10. Wallbaum, M. and S. Diepolder, "Benchmarking wireless lan location systems," *Proceedings of the 2005 Second IEEE International Workshop on Mobile Commerce and Services (WMCS 2005)*, 42–51, Munich, Germany, 2005.
11. Pahlavan, K. and P. Krishnamurthy, *Principles of Wireless Networks*, Prentice Hall PTR, New Jersey, 2002.
12. Kaemarungsi, K. and P. Krishnamurthy, "Properties of indoor received signal strength for WLAN location fingerprinting," *Proceedings of the 1st Annual International Conference on Mobile and Ubiquitous Systems: Networking and Services (MOBIQUITOUS04)*, 14–23, 2004.
13. Komar, C. and C. Ersoy, "Location tracking and location based service using IEEE 802.11 WLAN infrastructure," *European Wireless*, 24–27, 2004.
14. Tan, S., M. Tan, and H. Tan, "Multipath delay measurements and modeling for inter floor wireless communications," *IEEE Transactions on Vehicular Technology*, Vol. 49, No. 4, 1334–1341, Jul. 2000.
15. Jensen, F., "Bayesian graphical models," *Encyclopedia of*

Environmetrics, 2000.

16. Elnahrawy, E., R. Martin, W. Ju, P. Krishnan, and D. Madigan, "Bayesian indoor positioning systems," *Infocom. Citeseer*, 1217–1227, 2005.
17. Noble, W., "Getting started in probabilistic graphical models," *PLoS Comput. Biol.*, Vol. 3, No. 12, 252, 2007.
18. Geman, S., D. Geman, K. Abend, T. Harley, and L. Kanal, "Stochastic relaxation, Gibbs distributions and the Bayesian restoration of images*," *Journal of Applied Statistics*, Vol. 20, No. 5, 25–62, 1993.
19. Cowles, M., "Review of WinBUGS 1.4," The American Statistician, Vol. 58, No. 4, 330–336, 2004.
20. Ntzoufras, I., *Bayesian Modeling Using WinBUGS*, John Wiley & Sons Inc, 2009.
21. Hastings, W., "Monte Carlo sampling methods using Markov chains and their applications," *Biometrika*, Vol. 57, No. 1, 97–109, 1970.
22. Metropolis, N., A. Rosenbluth, M. Rosenbluth, A. Teller, E. Teller, et al., "Equation of state calculations by fast computing machines," *The Journal of Chemical Physics*, Vol. 21, No. 6, 1087, 1953.
23. Neal, R., "Slice sampling," *Annals of Statistics*, Vol. 31, No. 3, 705–741, 2003.
24. Neal, R. M., "Suppressing random walks in Markov chain Monte Carlo using ordered overrelaxation," *Learning in Graphical Models*, 205–225, 1998.
25. "Netstumbler." [Online]. Available: http://www.netstumbler.com/.
26. "inssider by metageek." [Online]. Available: http://www.metageek.net/.
27. "Winbugs." [Online]. Available: http://www.mrcbsu.cam.ac.uk/bugs/.